FABRICATION OF AN INTEGRATED OPTICAL SENSOR WITH HIGH SENSITIVITY AND HIGH DYNAMIC RANGE BASED ON A MACH-ZEHNDER INTERFEROMETRIC CONFIGURATION

D. Alexandre[1, 2, 3], J. Viegas[1, 2], L. Fernandes[1, 2], P.J. Moreira[1, 2#], A.M.P. Leite[2], J.L. Santos[1, 2], P.V.S. Marques[1, 2]

[1] UOSE, INESC-Porto, Rua do Campo Alegre 687, 4169-007 Porto, Portugal

[2] Departamento de Física, Faculdade de Ciências, Universidade do Porto, Rua do Campo Alegre 687, 4169-007 Porto, Portugal

[3] Universidade de Trás-os-Montes e Alto-Douro, Apartado 1013, 5001-801 Vila Real, Portugal

[#] Present address: Institute of Telecommunications, Campus de Santiago, 3810-193 Aveiro, Portugal

dalexandre@fc.up.pt

Abstract *— Integrated optics (IO) technology has been primarily used in optical communication applications but it is expanding fast into the field of optical sensing. In this work we report the fabrication of integrated devices using hybrid sol-gel technology and in particular its application in the fabrication of a refractive index integrated sensor based in a Mach-Zehnder interferometric configuration. In one of the interferometer arms, a analysis chamber is created by exposing the waveguide through the removal of the device cladding. On the same arm, two Bragg gratings with the same period are fabricated: one in the unprotected waveguide area and another in close proximity (cladded area); because of the different effective index in the two grating regions, two peaks are observed in reflection if the device is tested with a broadband source. Any change of the refractive index of the material filling the analysis chamber can be detected in two ways: by measuring the intensity of the interferometric output (at a wavelength different from the Bragg wavelength of the two gratings) or by measuring the spectrum of the reflected signal. The high sensitivity is obtained by measuring the interferometric output, while the high dynamic range can be achieved by measuring the reflected signal from the grating structures*

Key Words: Integrated Optics; Sol-Gel; Optical Sensors.

I INTRODUCTION

Integrated optical components based on silica-on-silicon technology have the potential to be a competitive solution for optical processing applications. They present low loss, are based on optical fibre matched waveguides resulting in low coupling loss, and offer the possibility to integrate optoelectronic functions on a same silicon platform. However, the high cost associated with their fabrication, which involves expensive equipment and a sophisticated high temperature processing route such as flame hydrolysis deposition (FHD), or chemical vapour deposition (CVD), together with reactive ion etching (RIE)[1] makes the final product more expensive. The introduction of organic polymer materials did overcome some of the disadvantages of the inorganic glasses, as they are processed at fairly low temperatures and, due to their matrix flexibility, can be used to deposit crack-free thick films in a single step. Silica-based organic-inorganic hybrid materials, produced by the sol-gel process, offer a number of useful properties, which result from the combination of inorganic and organic components. In particular, processing is performed at low temperatures and is compatible with existing conventional thin-film processing and large-scale wafer-level production.

Particular attention was paid to hybrid materials with an organic component of polymeric nature. Among them, ultraviolet (UV) photopolymerizable materials present a special interest for production of integrated optics devices. This functionality enables the irradiated material to become insoluble to solvents, such as alcohols, and the unexposed material to be simply removed by dissolution. This property simplifies the fabrication of microstructures, such as ridge waveguides, avoiding lengthy and high-cost processing by RIE

II FABRICATION

II.1 OPTICAL WAVEGUIDES

The waveguide core material was synthesized in a similar way to [5], [6], and [7], based on hydrolysis and polycondensation of methacryloxy-propyltrimethoxysilane (MAPTMS), to which zirconium propoxide (ZPO) mixed with methacrylic acid (MA) was added in a suitable molar proportion to attain the desired value of the refractive index. Soda-lime glass was used as substrates (refractive index of 1.513 at 632.8 nm). For the fabrication of functional devices through photoinscription, the films are then exposed through an amplitude mask for about 30 s to radiation of a 248 nm pulsed UV excimer laser.

It was found that the hybrid material does not need the addition of any kind of photoinitiator when exposed at this radiation wavelength, (contrary to what happens when exposed with sources at 365 nm), and shorter wavelength also enhances the photolithography spatial resolution. Figures 1 and 2 show two examples of structures made with this technique.

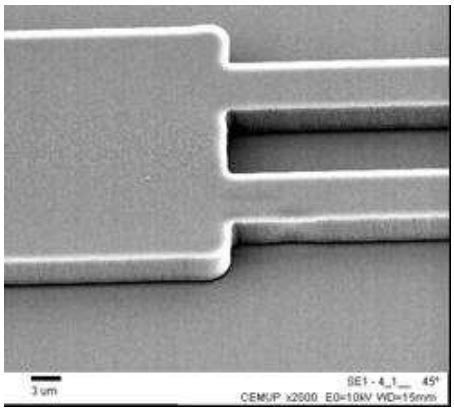

Figure 1. Electron microscope view of a multimode interferometer.

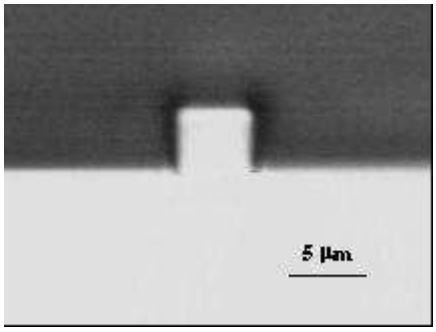

Figure 2. Channel waveguide with vertical sidewalls.

II.2 BRAGG GRANTING FABRICATION

Bragg gratings are periodic structures with sub-micron period that can be fabricated by two different processes both involving UV exposure through a phase mask[4]: the traditional process involves the fabrication of waveguides (cladded or not) and subsequent exposure through a phase mask for Bragg grating fabrication; the second process involves the simultaneous fabrication of the waveguide and of the Bragg grating.

In the case of simultaneously patterned waveguides and Bragg gratings, the exposure was performed through a combined, amplitude and phase, mask using the UV beam from a 248 nm pulsed excimer laser.

After exposure, the non-irradiated material was removed by dissolution in ethanol. A cladding layer with thickness between 13 µm and 15 µm, with the same refractive index of the substrate (corresponding to a ZrO_2 doping level of 20%) was deposited to ensure a symmetric waveguide index profile.

Both ends of the sample were carefully prepared to allow efficient coupling to optical fibres. The transmission and reflection spectra of the grating were acquired with an optical spectrum analyzer by coupling light from a wide spectrum source, operating in the 1.55 µm region, through an optical circulator.

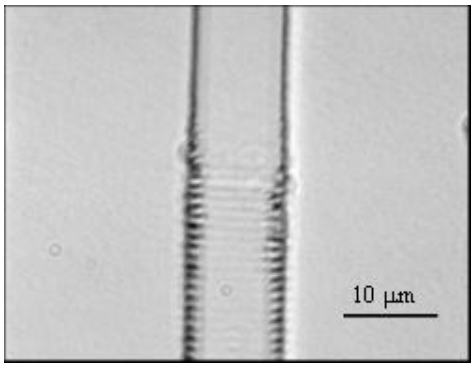

Figure 3. Optical image of a waveguide showing the transition between zones with and without grating.

II.3 INTEGRATED SENSOR

The integrated sensor fabricated is based in a Mach-Zehnder configuration, Figure 4.

In one of the arms, the waveguide core is exposed through a window defined in the cladding layer. This cavity is going to be filled up with the fluid where the refractive index changes are going to take place. Also on this region, a Bragg grating is

recorded on the waveguide section inside the analysis chamber and also in the waveguide section covered with a cladding. Alternatively, the grating can be written also in the other arm.

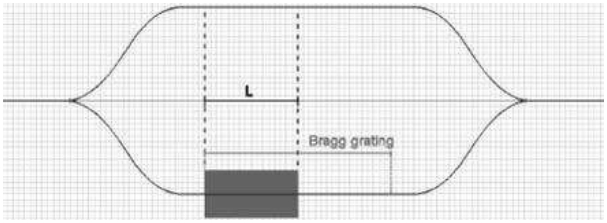

Figure 4. Schematic representation of the integrated refractive index sensor.

A device with this configuration will allow a high resolution measurement by using the interferometric output, while a high dynamic range can be obtained by measuring the reflected signal coming from the two gratings inscribed in the Mach-Zehnder interferometer. Two reflection peaks are expected, since the refractive index of the clad waveguide and of the waveguide in the analysis chamber are different. The presence of the two gratings can exclude temperature effects on the device; for example, if the refractive index changes within the cavity, only the peak corresponding to the grating on that region will shift its position. However, if there are any temperature changes, this peak will move also. The ambiguity can be removed since any temperature change can also affect the grating in the cladded region.

The fabrication procedure for the waveguides is the same as the one described in section II.1, and the definition of the analysis chamber is similar to the one employed in the production of the waveguides.

The Bragg grating fabrication procedure employed was different from the one described in section II.2 In this case, the waveguides were exposed and the non/polymerized regions removed. The grating was written in the waveguides by the conventional fabrication procedure employing a phase mask. The cladding layer was then deposited and the analysis chamber defined (marks were defined on the sample that allow the identification of the grating limits and subsequent alignment of the cavity with the grating). Alternatively, the gratings were written after the cladding processing and analysis chamber fabrication. In principle, the two processes will provide different results since in the later case the grating written outside the cavity region is written through the already deposited cladding layer, and therefore will be less efficient.

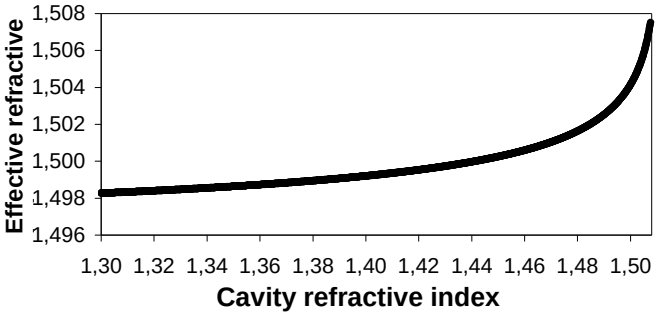

Figure 5. Calculated effective refractive index as a function of the refractive index in the analysis chamber.

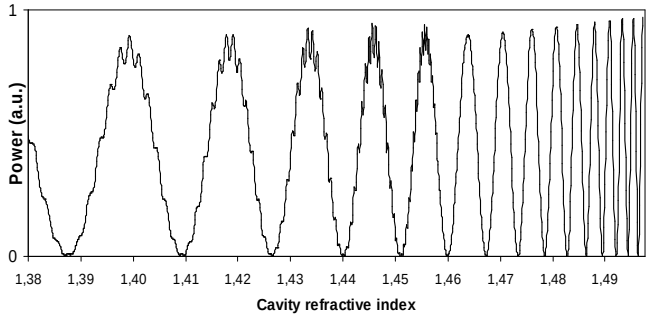

Figure 6. Interferometric output as a function of the refractive index filling the analysis chamber as simulated using beam propagation analysis (other data were L=5 mm, λ=1.55 μm, n_{subs}=1.4972, n_{core}=1.5076).

The two aspects, noticeable from Figures 5 and 6 are that the effective refractive index change is non-linear (and therefore the resolution will change) and that for fluids with low refractive index the waveguide becomes multimode and therefore the interferometric output is modulated.

The fabricated devices were tested with a tunable laser source (interferometric output) and with a broadband erbium source (reflected signal output). The reflected signal was measured in the drop port of an optical circulator placed at the device input.

When different liquids are inserted over the sample cavity there is a clear shift of the reflection peak, as represented by Figure 7 for two different liquids (after stabilization). A difference of about 0.5 nm between the centre wavelength reflection for the cavity filed with air and the centre wavelength for the cavity field with index matching oil was found. This difference represents a variation in the effective refractive index of about 5×10^{-4}. This refractive index changes seen when index matching fluid was employed agree well with the results of the calculations of the gratings wavelength shift,

following the calculation of the effective refractive index changes.

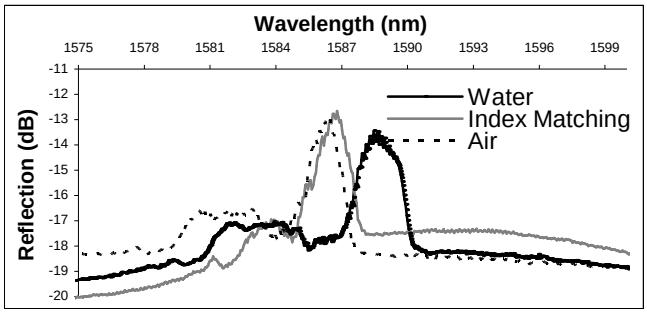

Figure 7. Reflected spectra of a 528 nm period Bragg gratings in a linear waveguide, when the cavity is filled with different fluids.

However, the shifts obtained with water cannot be explained by the results obtained for the calculation of the effective refractive index values. Also, the effect was not immediate; it takes some time until the peaks stabilize their position.

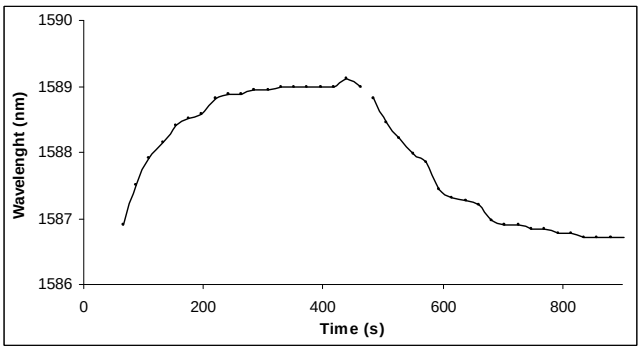

Figure 8. Centre wavelength of the reflected spectrum of a 528 nm Bragg grating in a linear waveguide during the stabilization time when the cavity is filed with water and dried afterwards.

Figure 8 shows the shift of the centre wavelength of the Bragg grating reflected spectrum during time. From the same figure it is clear that the peak returns to the initial position after the water has been removed from the cavity, so the process is fully reversible.

These results indicated that a diffusion process takes place and that it depends on the liquid solution employed, that being particularly noticed in the case of aqueous solutions.

When the interferometric output is monitored after the cavity is filled with water, the result is what is represented in figure 9.

The effect of water absorption and de-absorption through heating was already reported in [5] in the context of propagation loss analysis and its reduction at 1.5 μm.

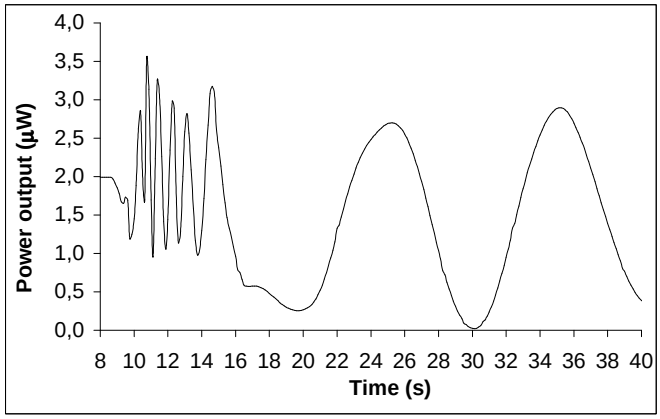

Figure 9. Interferometric output immediately after insertion of a water droplet in the analysis chamber.

III CONCLUSIONS

This paper describes the fabrication of an integrated sensor based in a Mach-Zehnder interferometer with two Bragg gratings fabricated in the arms. Refractive index changes can be detected either by measuring the wavelength shifts of the Bragg gratings or by monitorization of the interferometric output. It was noticed that the response time was affected by the diffusion of the water into the sol-gel waveguide core. However, this effect is responsible for an enhanced shift of the Bragg wavelength. This effect was only noticed for aqueous solutions. The Bragg gratings have to be optimized in terms of length and coupling strength in order to have very sharp wavelength band that allow an easy detection of minimal shifts.

REFERENCES

[1] M. Kawachi, "Recent progress in silica-based planar lightwave circuits on silicon", *IEE Proc. Optoelectron*., 143, pp. 257-262, 1996.

[2] P. J. Moreira, P. V. S. Marques, A. P. Leite, "Hybrid Sol-Gel Channel Waveguide Patterning Using Photoiniciator-Free Materials", *IEEE Photonics Technology Letters*, vol. 17, 2, pp 399-401, 2005.

[3] P. J. Moreira, P. V. S. Marques, A. P. Leite, "Hybrid silica sol-gel symmetric buried channel waveguide on silicon", *SPIE's Photonics European Symposium*, Strasbourg, France, Apr. 26-30, 2004

[4] R. Kashyap, "Fiber Bragg Gratings", *Optics and Photonics*, Academic Press, 1999

[5] O. Soppera, P. J. Moreira, P. V. S. Marques, and A. P. Leite, "Influence of temperature and environment humidity on the transmission spectrum of sol–gel hybrid channel waveguides", *Optics Communications*, 27, pp. 430–435, 2007